Rapid Communications

Disorder recovers the Wiedemann-Franz law in the metallic phase of VO_2

Lei Jin,[1,2] Steven E. Zeltmann,[1,3] Hwan Sung Choe,[1,2] Huili Liu,[1,2] Frances I. Allen,[1,3] Andrew M. Minor,[1,3] and Junqiao Wu[1,2,*]

[1]*Department of Materials Science and Engineering, University of California, Berkeley, California 94720, USA*
[2]*Materials Sciences Division, Lawrence Berkeley National Laboratory, Berkeley, California 94720, USA*
[3]*National Center for Electron Microscopy, Molecular Foundry, Lawrence Berkeley National Laboratory, Berkeley, California 94720, USA*

(Received 28 May 2020; revised 3 July 2020; accepted 6 July 2020; published 22 July 2020)

At temperatures higher than 341 K, vanadium dioxide (VO_2) is a strongly correlated metal with resistivity exceeding the Mott-Ioffe-Regel limit. Its electronic thermal conductivity is lower than that predicted by the Wiedemann-Franz (WF) law, and can be explained by nonquasiparticle transport where heat and charge currents follow separate diffusive modes. In contradiction, the Wiedemann-Franz law is a direct consequence of quasiparticle transport where charge carriers are elastically scattered. In this work, we enhance elastic electron scattering in VO_2 by introducing atomic disorder with ion irradiation. A gradual and eventually full recovery of the WF law is observed at high defect densities. This observation provides an example that connects hydrodynamic quasiparticle transport to nonquasiparticle transport in metallic systems.

DOI: 10.1103/PhysRevB.102.041120

The Wiedemann-Franz (WF) law predicts that the electronic thermal conductivity of a metal (κ_e) is proportional to the product of its electrical conductivity (σ) and absolute temperature (T). The proportionality constant in this relation is the Lorenz number (L), and is equal to the Sommerfeld value, $L_0 = \frac{\pi^2}{3}(\frac{k_B}{e})^2$, when the conducting charge carriers can be described as long-lived quasiparticles experiencing predominantly elastic scattering. These conditions are well satisfied in normal metals above their Debye temperatures, such as in Cu and Al, where quasielastic electron-phonon or elastic electron-impurity scattering dominates [1]. A deviation of L away from L_0 usually implies the existence of inelastic electron scattering processes, such as small-angle electron-phonon scattering at low temperatures, electron-electron scattering in the hydrodynamic regime, or a complete failure of the quasiparticle model where non-Fermi-liquid physics must be considered [2–8]. An example of the latter is the metallic (M) phase of vanadium dioxide (VO_2) [3], a strongly correlated electron material with a well-known metal-insulator transition (MIT) at $T = 341$ K. The M phase of VO_2 is a "bad" metal [9,10], where the quasiparticle Drude model fails and conduction electrons are scattered by inelastic yet momentum-conserving electron-electron interactions. It has been experimentally observed that charge and heat currents in the material are transported according to separate diffusive modes and that the Lorenz number is suppressed by nearly one order of magnitude below the Sommerfeld value [3].

On the other hand, the WF law has been shown to be restored in Fermi liquids by adding elastic, electron-impurity scattering to suppress the originally dominating inelastic, electron-phonon scattering [11]. This is consistent with the fact that to experimentally observe the breakdown of the WF law in the hydrodynamic regime, samples must be ultrapure with a negligible density of impurities [5,12]. It is intriguing to extend this defect effect of quasiparticle transport to "bad" metals with nonquasiparticle transport. In this work, we show that even in a system without long-lived quasiparticles, the artificially introduced point defects scatter electrons elastically to restore the Lorenz number toward the Sommerfeld value, the hallmark of quasiparticle transport.

Here, VO_2 nanowires were grown using the vapor transport method published previously [13]. The nanowires are single crystalline and have a rectangular cross section of thickness ranging from tens of nanometers to a few micrometers. Point defects were introduced into the VO_2 nanowires by He ion irradiation using a Zeiss Orion NanoFab He ion microscope operated at 30 kV. The point defects (vacancies and interstitials of V and O) were efficiently created in the VO_2 through the nuclear stopping process. The VO_2 nanowires chosen for this study have thicknesses less than the projected range of the He ions of 160 nm, as predicted by Monte Carlo simulations, using the Stopping and Range of Ions in Matter (SRIM) program [14]. The SRIM simulations show that most (>80%) of the He ions transmit the VO_2 nanowires leaving behind a uniform distribution of point defects. The ratio of the number of trapped He ions to the number of irradiation-induced vacancies in the nanowires is less than 1%. During the irradiation runs, care was taken to use low ion currents (<1 pA) in order to minimize any thermal effects and hydrocarbon deposition.

The thermal and electrical conductivity of the VO_2 nanowires were measured using suspended micropad devices as shown in Fig. 1(a). The device consists of two SiN_x pads that are suspended by long and flexible thin SiN_x arms, with Pt coils patterned onto both micropads to function as a microscale resistive heater and thermometer. A VO_2 nanowire was dry transferred using a micromanipulator onto the two pads to bridge them. Focused ion beam (FIB) induced

*wuj@berkeley.edu

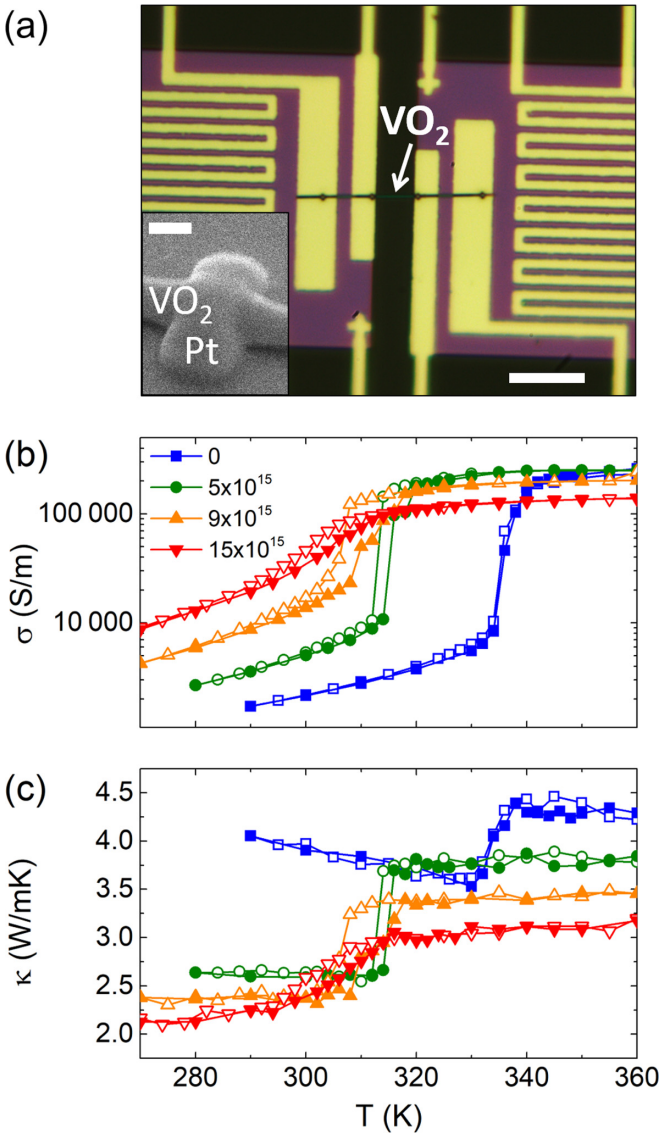

FIG. 1. Electrical and thermal conductivity of VO_2 nanowires across the metal-insulator transition. (a) Optical image of two suspended micropads bridged by a VO_2 nanowire. Scale bar is 10 μm. Inset: SEM image of the nanowire bonded to the electrode by FIB-induced Pt deposition. Scale bar is 200 nm. (b) Electrical and (c) thermal conductivity of a 140-nm-thick VO_2 nanowire irradiated with He ions at accumulated doses of 0, 5, 9, and 15 $\times$ 10^{15} ions/cm^2. The data collected during both heating (filled symbols) and cooling (open symbols) are shown for each dose.

deposition was then used to deposit a small amount of Pt onto the nanowire at four locations to bond it to the underlying four electrodes. A scanning electron microscope (SEM) image of one of these Pt deposits is shown in the inset of Fig. 1(a). Both electrical and thermal contact resistance are found to be negligible after the Pt deposition [3]. Heat currents flow through the VO_2 nanowire from the heating pad to the sensing pad, raising the temperature of the latter, which was used to determine the thermal conductivity of the nanowire after careful calibration. The measurements were taken in high vacuum with a pressure less than 10^{-6} Torr. Thermal conductance due to radiative and convective heat transfer is negligible compared to that of heat conduction through the nanowire. Electrical conductivity was measured simultaneously with the four-probe configuration using the electrodes prepatterned onto the suspended pads, which also allow measurement of the Seebeck coefficient (S). Further details on the fabrication process and measurements using the suspended micropad devices can be found elsewhere [3,15]. The experimental setup described maximally eliminates external strain, which strongly affects the MIT of VO_2 [16,17], and more importantly, both the heat and charge currents are measured along the same direction of the sample (the [100] direction in monoclinic, namely, the [001] direction in the rutile coordinates [13]), which is critically important for the evaluation of the Lorenz number.

The electrical and thermal conductivities of the irradiated VO_2 nanowires are shown in Figs. 1(b) and 1(c), respectively. Although many more nanowires were measured (shown later), the data in Figs. 1(b) and 1(c) were collected from a single nanowire undergoing multiple steps of irradiation. The measurements were taken immediately after the He ion irradiation to minimize sample degradation such as oxidation of the defected VO_2. The MIT persists in VO_2 even after 1.5×10^{16} ions/cm^2 dose of irradiation, although the sharpness of the MIT and conductivity ratio between the metallic and insulating (I) phases are reduced. The temperature of the MIT (T_{MIT}) is reduced from 341 K for the pristine state to near 300 K for the heavily irradiated state. In addition, the T_{MIT} values obtained from the electrical and thermal measurements are in very good agreement. It can be seen that the electrical conductivity (σ) of the I phase increases while that of the M phase decreases as a result of the irradiation. This trend is consistent with many other works investigating effects of oxygen vacancies in VO_2 [18–23]. As O vacancies are created by irradiation and are expected to be electron donors in VO_2, σ increases in the I phase. In the M phase, such electron doping has negligible effect; instead, scattering of conductive electrons by the newly created O vacancies and other point defects reduces σ (discussed in further detail below). In contrast to σ, the thermal conductivity (κ) is reduced by irradiation in both the I and M phases. After irradiation, the slope of κ in the I phase over temperature becomes less negative. This implies stronger phonon-impurity scattering arising with more irradiation-induced defects, as the impurity scattering rate is almost T independent compared to the umklapp scattering. The surface scattering in transport measurements is negligible as the mean free path (MFP) of both electron and phonon (discussed later) in VO_2 is much less than the thicknesses of our nanowires.

To determine the irradiation damage in the VO_2 nanowires, selected area electron diffraction (SAED) patterns were acquired using an FEI Themis transmission electron microscope (TEM) operated at 300 kV. For this, single nanowires were placed onto lacey carbon TEM supports and targeted areas were irradiated to the desired doses. Figure 2(a) shows a low-resolution TEM image of a nanowire with two regions marked top and bottom that were irradiated using doses of 5×10^{16} and 1×10^{15} ions/cm^2, respectively (the higher dose corresponds to the maximum irradiation dose investigated in this study). The central portion of the nanowire was not irradiated. The SAED results corresponding to all three regions are presented in Figures 2(b)–2(d) and show constantly sharp and

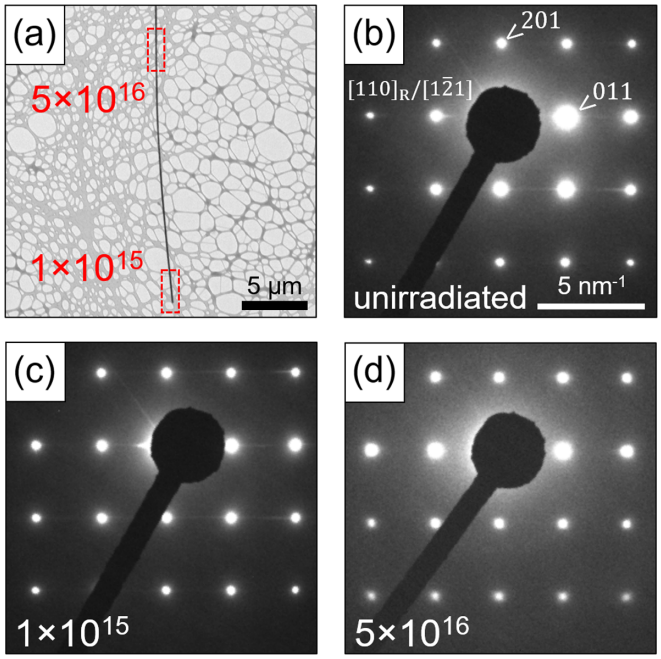

FIG. 2. (a) Low-resolution TEM image showing a VO_2 nanowire irradiated with He ions to doses of 1×10^{15} and 5×10^{16} ions/cm^2 in the regions marked at the bottom and top. respectively. The central region remains pristine. SAED patterns are shown for the (b) pristine, (c) 1×10^{15} ions/cm^2 irradiated, and (d) 5×10^{16} ions/cm^2 irradiated regions of the VO_2 nanowire. The survival of the sharp SAED pattern to the highest irradiation dose indicates that the He ion irradiation of VO_2 damages the lattice by generating point defects, without degrading the crystallinity.

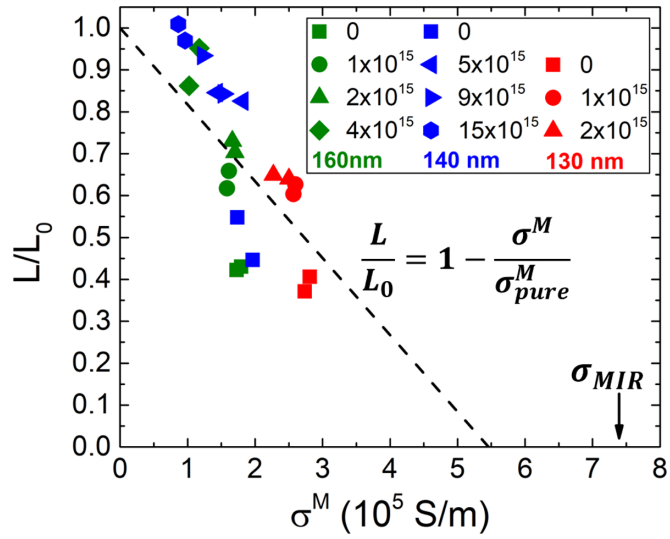

FIG. 3. Normalized Lorenz number L/L_0 [as defined in Eq. (1)] for three VO_2 nanowires of different thicknesses (labeled) for different irradiation doses (in units of ions/cm^2) as a function of σ for the M phase just above the MIT, showing the recovery of L upon introduction of defects toward the Sommerfeld value ($L_0 = 2.44 \times 10^{-8}\,\mathrm{W\,\Omega\,K^{-2}}$) of a normal metal. The error range of the L/L_0 data points is about ± 0.1. The MIR limit of σ is indicated with an arrow, proving that all data exceed the σ_{MIR}.

clean patterns in all cases, indicating that the VO_2 nanowires remain fully single crystalline for all the irradiation doses used in this work. This confirms that the irradiation creates point defects without generating extended defects or causing amorphization. Moreover, SRIM simulations show that the defect density is very small (around 0.45 at.%) in irradiated VO_2 nanowires at the highest dose (5×10^{16} ions/cm^2).

In Ref. [3], using inelastic x-ray scattering combined with first-principles calculation, Lee *et al.* showed that the lattice component of thermal conductivity (κ_l) for VO_2 remains almost unchanged when the material transitions between the I and the M phases at the MIT. That is, $\kappa_l^I \approx \kappa_l^M$ near T_{MIT}. This is because, although the M phase has a more anharmonic lattice [24] and hence shorter phonon mean free path for phonon modes $<\sim$10 meV, the I phase has many more optical phonon modes with very low group velocities due to its doubled unit cell [25], lowering the MFPs. As a result, the average MFPs for the M and I phases are 5.18 and 5.86 nm, respectively, very close to each other. The approximation $\kappa_l^I \approx \kappa_l^M$ improves further when boundary and impurity scattering of phonons are included via Matthiessen's rule [3], because such scattering of thermal phonons is not drastically different in the M and I phases. This effect provides a convenient method to evaluate the Lorenz number for the M phase of VO_2, because according to $\kappa = \kappa_l + \kappa_e$ and the fact that κ_e is nearly zero in the I phase, κ_e^M at T_{MIT} can be estimated by $\kappa_e^M = \kappa^M - \kappa_l^M \approx \kappa^M - \kappa^I$. That is, the jump in the measured total thermal conductivity at T_{MIT} is primarily attributed to the electronic thermal conductivity in the M phase. We will adopt this method to estimate κ_e^M in all the VO_2 samples, and use it to evaluate the Lorenz number near T_{MIT} according to

$$\frac{L}{L_0} = \frac{\kappa_e^M}{L_0 \sigma^M T} \approx \frac{\kappa^M - \kappa^I}{L_0 \sigma^M T}. \tag{1}$$

Figure 3 shows the measured L/L_0 values at the respective T_{MIT}'s for three different VO_2 nanowires of different thicknesses, each of which was irradiated with doses ranging from zero to 1.5×10^{16} ions/cm^2. Two data points are shown for each measurement, calculated from data collected in the heating and cooling steps, respectively. L/L_0 all increase as a function of irradiation dose for all the nanowires. Moreover, plotting L/L_0 as a function of σ^M at T_{MIT} reveals a generally linear trend for all the data, regardless of the different samples and different doses. L/L_0 approaches 1, namely, the WF law is fully recovered with $L = L_0$, at the highest irradiation dose (1.5×10^{16} ions/cm^2). Interestingly, this dose is also the maximum dose under which the MIT can survive: Irradiation at higher doses completely destroys the MIT (i.e., no longer showing an abrupt change in electrical conductivity, not shown here), even though according to the TEM results the sample is still crystalline. The coincidence of $L = L_0$ with the disappearance of the MIT points to a fundamental connection between the violation of the WF law and electron correlation in VO_2.

The M phase of VO_2 hosts electrical conduction that is beyond the Mott-Ioffe-Regel (MIR) resistivity limit [26] derived from the Heisenberg uncertainty principle for momentum and position [27]. In electronic transport carried by quasiparticles, the MIR limit requires that the MFP of quasiparticles is

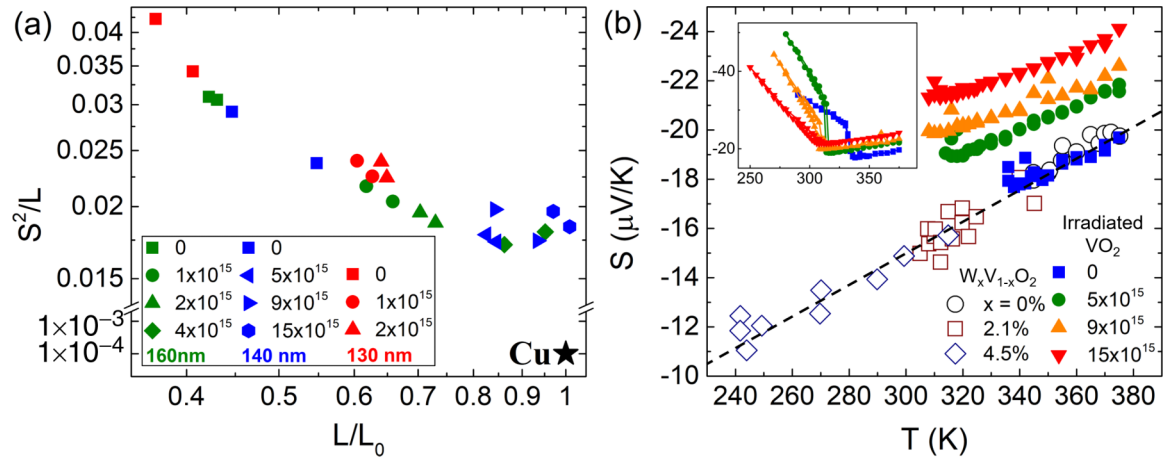

FIG. 4. Effects of impurity scattering in irradiated VO_2. (a) The electronic figure of merit (S^2/L) at T_{MIT} decreases with L/L_0. The nonquasiparticle transport in the M phase of VO_2 manifests in both the unusually high S^2/L value as well as the lower-than-unity L/L_0 value, in contrast to normal metals such as Cu. (b) M-phase Seebeck coefficient of a 140-nm-thick VO_2 nanowire after irradiation to different doses, compared with that of W-doped VO_2 nanowires adopted from Lee *et al.* [3]. The upward shift in the Seebeck coefficient upon irradiation reflects increasingly stronger scattering of itinerant electrons by ionized impurities.

longer than their de Broglie wavelength. Long-lived quasiparticles cannot exist in systems with resistivity higher than the MIR limit, and non-Fermi-liquid physics must be considered. Resistivity linear in temperature beyond the MIR limit has been reported in VO_2 [9,10]. Given the electron concentration of $n \sim 1 \times 10^{23}\,\mathrm{cm}^{-3}$ obtained by Hall-effect measurements from bulk single-crystalline VO_2 [28], we estimate the MIR limit of M-phase VO_2 to be $\sigma_{MIR} \sim 7 \times 10^5$ S/m using the formula given by Hartnoll [27]. σ^M of all VO_2 nanowires are beyond (i.e., lower than) the MIR limit, as shown in Fig. 3, clear evidence of nonquasiparticle electronic transport.

For nonquasiparticle transport, it has been theoretically shown that L can be much smaller than L_0, because in this case the charge and heat currents are carried with separate diffusive modes, and the ratio of their conductivities has no reason to be equal to L_0 [4,27]. Indeed, as shown in Fig. 3, L/L_0 is measured to be much lower than 1 in pristine VO_2, consistent with the previous report by Lee *et al.* [3]. Another parameter that indicates the lack of quasiparticle transport is that the dimensionless electronic figure of merit, $S^2/L = S^2\sigma^M T/\kappa_e^M$, is unusually large. The parameter S^2/L is theorized [1] to be very low for quasiparticle transport in a Fermi liquid, as S is suppressed by the factor $k_B T/E_F$. Indeed, it is on the order of 10^{-4} for conventional metals such as Cu [29]. In contrast, in the metallic phase of VO_2, values of S^2/L are all between 10^{-2} and 10^{-1}, as shown in Fig. 4(a).

In the framework of quasiparticle transport, charge currents can only be degraded in momentum-nonconserving scattering processes of charge carriers, whereas electronic heat currents can also be degraded by energy-nonconserving (i.e., inelastic) scattering of charge carriers [6,30]. Therefore, the WF law can be violated with $L/L_0 < 1$ at low temperatures where inelastic electron-phonon scattering becomes significant [30]. The breakdown of the WF law has also been reported in quasiparticle transport in hydrodynamic Fermi liquids [6,12]. In the hydrodynamic regime, electron-electron interactions dominate, and the Lorenz number is lowered. This is because the charge current is not relaxed by the electron-electron interactions (as they are momentum conserving) whereas the heat current is (because this can be inelastic). For these two scenarios of quasiparticle transport where $L < L_0$, it has been shown that disorder raises L toward L_0 and restores the WF law [11,12,30], because the MFP of both charge and heat transport are simultaneously and proportionally degraded by the additional, momentum-nonconserving, impurity scattering of electrons.

However, such theory of disorder effects in nonquasiparticle transport has not been established [12]. Despite many fundamental differences, strong electron-electron interactions exist in both quasiparticle transport of hydrodynamic Fermi liquids and nonquasiparticle transport of non-Fermi liquids. We thus "borrow" the results obtained when treating disorder in hydrodynamic Fermi liquids [12] to discuss defect scattering in nonquasiparticle transport. In this case, it has been shown that the Lorenz ratio is approximated by

$$\frac{L}{L_0} \approx \frac{\Gamma}{\Gamma + \gamma}, \tag{2}$$

where γ is the electron-electron scattering rate, and Γ is the electron-defect scattering rate. We also adopt the relaxation time approximation and relate the scattering rate to electrical conductivity as $\sigma^M \propto \tau$, where τ is the relaxation time and is the reciprocal of the scattering rate. It is straightforward to show that

$$\frac{L}{L_0} \approx 1 - \frac{\sigma^M}{\sigma^M_{\mathrm{pure}}}, \tag{3}$$

where σ^M_{pure} is the ideal electrical conductivity in defect-free samples. As shown in Fig. 3, L/L_0 has a nearly linear dependence on σ^M consistent with Eq. (3). Therefore, the disorder indeed restores the WF law, and L/L_0 can be viewed as a measure of the fraction of disorder scattering in this "bad" metal.

It is noted that the average separation between neighboring point defects from the He ion irradiation is about a few nanometers according to simulations using the SRIM program.

This is much longer than the MFP of charge carriers in the M phase of pristine VO_2, which is about $1 \sim 2$ Å estimated assuming the Drude model. It is surprising that such sparsely distributed point defects can significantly reduce σ of M-phase VO_2, by more than 50% (Fig. 3). The MFP resulting from defect scattering is inversely proportional to not only the density of defects, but also to the scattering cross section. It has been reported that atomic impurities show a larger scattering cross section area in "bad" metals than in normal metals [31]. The unusually large electron-defect scattering cross section in a "bad" metal may only be explained by the correlated nature of the interacting electrons [32]. Consequently, the significant reduction in σ^M by irradiation implies anomalously strong electron-defect interactions in the M phase of VO_2.

Further evidence of significant change in the electron scattering mechanism by defects is the behavior of the Seebeck coefficient. Derived from the linearized Boltzmann transport equation for parabolic bands, the Seebeck coefficient of a metallic system can be written as

$$|S| = \frac{k_B}{e}\frac{\pi^2}{3}\frac{k_B T}{E_F}\left(\frac{3}{2} + r\right), \tag{4}$$

where a power law energy dependence for the relaxation time is assumed: $\tau(E) \propto E^r$, and r is the power index [33–35]. For elastic scattering, r varies from $-1/2$ for acoustic phonon scattering to $3/2$ for ionized impurity scattering. For inelastic scattering [34], the power law energy dependence of τ fails and r is not a constant. As Fig. 4(b) shows, the values of S agree very well with Lee *et al.* [3] for pristine VO_2, but increase for irradiated samples while retaining the linear dependence on T. This is in stark contrast to the behavior of S for W-doped VO_2 measured by Lee *et al.* In the latter case, S collapses onto the same T dependence as that of the pristine VO_2, suggesting that W dopants do not change the electron scattering mechanism in VO_2. In the absence of a defect theory for nonquasiparticle transport, we discuss the behavior of S in the framework of Eq. (4) in the relaxation time approximation. In Fig. 4(b), the overall upward shifting in $S(T)$ after irradiation implies higher r values, which is consistent with the increased importance of defects to provide more ionized impurity scattering in the electron scattering process.

In conclusion, we show empirical validity of a quasiparticle transport model in a system where long-lived quasiparticles are clearly absent. The evidence is restoration of the electronic thermal conductivity to the quasiparticle value in a metallic system where it is originally suppressed by the absence of quasiparticles. We introduce atomic-level point defects as elastic scattering centers for conduction electrons using energetic particle irradiation. The increased weight of elastic scattering fully recovers the Wiedemann-Franz law at high defect densities. This finding bridges the decoupled electrothermal transport in the nonquasiparticle regime to a coupled one in the more conventional, quasiparticle regime. In addition, ion irradiation is shown to be an effective tool for not only modulating the conductivities, but also controlling the conduction mechanism of electronic and thermal currents.

This work was supported by U.S. NSF Grant No. DMR-1608899. The device fabrication part was supported by the Center for Energy Efficient Electronics Science (NSF Award No. 0939514). Work at the Molecular Foundry was supported by the Office of Science, Office of Basic Energy Sciences, of the U.S. Department of Energy under Contract No. DE-AC02-05CH11231. S.E.Z. was supported by STROBE, an NSF Science and Technology Center, under Grant No. DMR 1548924.

[1] N. W. Ashcroft and N. D. Mermin, *Solid State Physics* (Saunders College Press, Philadelphia, 1976).
[2] M. A. Tanatar, J. Paglione, C. Petrovic, and L. Taillefer, Science **316**, 1320 (2007).
[3] S. Lee, K. Hippalgaonkar, F. Yang, J. Hong, C. Ko, J. Suh, K. Liu, K. Wang, J. J. Urban, X. Zhang, C. Dames, S. A. Hartnoll, O. Delaire, and J. Wu, Science **355**, 371 (2017).
[4] R. Mahajan, M. Barkeshli, and S. A. Hartnoll, Phys. Rev. B **88**, 125107 (2013).
[5] J. Crossno, J. K. Shi, K. Wang, X. Liu, A. Harzheim, A. Lucas, S. Sachdev, P. Kim, T. Taniguchi, K. Watanabe, T. A. Ohki, and K. C. Fong, Science **351**, 1058 (2016).
[6] A. Principi and G. Vignale, Phys. Rev. Lett. **115**, 056603 (2015).
[7] N. Wakeham, A. F. Bangura, X. Xu, J.-F. Mercure, M. Greenblatt, and N. E. Hussey, Nat. Commun. **2**, 396 (2011).
[8] J. Dong, Y. Tokiwa, S. L. Bud'ko, P. C. Canfield, and P. Gegenwart, Phys. Rev. Lett. **110**, 176402 (2013).
[9] P. B. Allen, R. M. Wentzcovitch, W. W. Schulz, and P. C. Canfield, Phys. Rev. B **48**, 4359 (1993).
[10] M. Qazilbash, K. Burch, D. Whisler, D. Shrekenhamer, B. Chae, H. Kim, and D. Basov, Phys. Rev. B **74**, 205118 (2006).
[11] U. Mizutani, *Introduction to the Electron Theory of Metals* (Cambridge University Press, Cambridge, 2001).
[12] A. Lucas and S. D. Sarma, Phys. Rev. B **97**, 245128 (2018).
[13] C. Cheng, K. Liu, B. Xiang, J. Suh, and J. Wu, Appl. Phys. Lett. **100**, 103111 (2012).
[14] J. F. Ziegler, M. D. Ziegler, and J. P. Biersack, Nucl Instrum. Methods Phys. Res., Sect. B **268**, 1818 (2010).
[15] L. Shi, D. Li, C. Yu, W. Jang, D. Kim, Z. Yao, P. Kim, and A. Majumdar, J. Heat Transfer **125**, 881 (2003).
[16] S. Lee, C. Cheng, H. Guo, K. Hippalgaonkar, K. Wang, J. Suh, K. Liu, and J. Wu, J. Am. Chem. Soc. **135**, 4850 (2013).
[17] J. Cao, E. Ertekin, V. Srinivasan, W. Fan, S. Huang, H. Zheng, J. Yim, D. Khanal, D. Ogletree, J. Grossman, and J. Wu, Nat. Nanotechnol. **4**, 732 (2009).
[18] J. G. Ramirez, T. Saerbeck, S. Wang, J. Trastoy, M. Malnou, J. Lesueur, J.-P. Crocombette, J. E. Villegas, and I. K. Schuller, Phys. Rev. B **91**, 205123 (2015).
[19] D. Lee, B. Chung, Y. Shi, G.-Y. Kim, N. Campbell, F. Xue, K. Song, S.-Y. Choi, J. P. Podkaminer, T. H. Kim, P. J. Ryan, J.-W. Kim, T. R. Paudel, J.-H. Kang, J. W. Spinuzzi, D. A. Tenne, E. Y. Tsymbal, M. S. Rzchowski, L. Q. Chen, J. Lee, and C. B. Eom, Science **362**, 1037 (2018).

[20] Z. Zhang, H. Guo, W. Ding, B. Zhang, Y. Lu, X. Ke, W. Liu, F. Chen, and M. Sui, Nano Lett. **17**, 851 (2017).
[21] S. Fan, L. Fan, Q. Li, J. Liu, and B. Ye, Appl. Surf. Sci. **321**, 464 (2014).
[22] J. Jeong, N. Aetukuri, T. Graf, T. D. Schladt, M. G. Samant, and S. S. Parkin, Science **339**, 1402 (2013).
[23] Z. Zhang, F. Zuo, C. Wan, A. Dutta, J. Kim, J. Rensberg, R. Nawrodt, H. H. Park, T. J. Larrabee, X. Guan, Y. Zhou, S. M. Prokes, C. Ronning, V. M. Shalaev, A. Boltasseva, M. A. Kats, and S. Ramanathan, Phys. Rev. Appl. **7**, 034008 (2017).
[24] J. D. Budai, J. Hong, M. E. Manley, E. D. Specht, C.W. Li, J. Z. Tischler, D. L. Abernathy, A. H. Said, B. M. Leu, L. A. Boatner, R. J. McQueeney, and O. Delaire, Nature **515**, 535 (2014).
[25] V. Eyert, Ann. Phys. **11**, 650 (2002).
[26] M. Gurvitch, Phys. Rev. B **24**, 7404 (1981).
[27] S. A. Hartnoll, Nat. Phys. **11**, 54 (2015).
[28] W. Rosevear and W. Paul, Phys. Rev. B **7**, 2109 (1973).
[29] S. Kasap, *Thermoelectric Effects in Metals: Thermocouples* (University of Saskatchewan, Canada, 2001).
[30] A. Lavasani, D. Bulmash, and S. D. Sarma, Phys. Rev. B **99**, 085104 (2019).
[31] T. Chien, Z. Wang, and N. P. Ong, Phys. Rev. Lett. **67**, 2088 (1991).
[32] H. Alloul, J. Bobroff, M. Gabay, and P. Hirschfeld, Rev. Mod. Phys. **81**, 45 (2009).
[33] X. Wang, V. Askarpour, J. Maassen, and M. Lundstrom, J. Appl. Phys. **123**, 055104 (2018).
[34] N. Preissler, O. Bierwagen, A. T. Ramu, and J. S. Speck, Phys. Rev. B **88**, 085305 (2013).
[35] J. Suh, K. M. Yu, D. Fu, X. Liu, F. Yang, J. Fan, D. J. Smith, Y. H. Zhang, J. K. Furdyna, C. Dames, W. Walukiewicz, and J. Wu, Adv. Mater. **27**, 3681 (2015).